Quantitative spatial phenotyping of the tumor microenvironment in NSCLC tissue microarray cores using 6-plex multiplex imaging technology and AI-powered phenotyping analysis

Nicole Couper[1], Bethany Remeniuk[2], Karen McClymont[1], Bei Hopkins[2], Natalie Monteiro[2], Lorcan Sherry[1], Gabriel Reines March[1], Darren Locke[2]

[1]OracleBio Ltd, Glasgow, Scotland, UK [2]Akoya Biosciences, Inc, Marlborough, Massachusetts, USA

Email contact: nicole.couper@oraclebio.com | dlocke@akoyabio.com

Background

Non-small cell lung cancer (NSCLC) patients can have impaired immune responses within the tumor microenvironment (TME), leading to tumor growth progression and poorer prognosis. Accurate cell phenotyping combined with spatial phenotyping can provide a deeper understanding of complex cellular interactions underpinning the tumor-immune response.

The aim of this study was to utilize Akoya's multiplexed imaging technology and associated Artificial Intelligence (AI)-powered image analysis methods to identify populations of immune cells and their functional status, as well as their interactions within the tumor microenvironment in a set of NSCLC tissue cores from patients treated with first-line standard-of-care chemotherapy and second-line immuno-oncology treatment. Patient groups included Responders (R; full responders, partial responders, and stable disease, n=22 cores) and Non-Responders (NR; n=16 cores).

Methods

Formalin-fixed paraffin-embedded (FFPE) NSCLC tissue microarrays (TMA), comprised of n=38 cores containing a range of carcinomas and pathological Tumor-Node-Metastasis (pTNM) stages, were stained on a Leica Bond RX™ using the Akoya PhenoCode™ Signature Immuno-contexture Human Protein Panel. This panel includes markers for immune cells (CD8 and FoxP3), macrophages (CD68), checkpoint inhibitors (PD-1 and PD-L1) and PanCK as a tumor indicator. Stained TMAs were scanned at 20x magnification on a PhenoImager® HT multiplexed imaging system.

N=36 cores passed image QC and progressed to image analysis using Visiopharm software. Deep Learning algorithms were developed to segment each core into tumor and stroma regions of interest (ROI) and to accurately detect and classify different cell populations. A DeepLabv3+ neural network was used to develop the classifier using DAPI and PanCK. A customized cell analysis algorithm was trained using a U-Net neural network to detect individual cell lineages and subsequent phenotypes of interest (Figures 1 & 2). A hierarchical approach detected CD8, CD68, tumor cells, and then DAPI cells. Staining variance for CD8, CD68, and DAPI was overcome by generating training labels for the 3 cell types across the TMA cores and using the 3 markers as input channels for Deep Learning training.

Cell object data *per* core was exported from Visiopharm software and spatial analysis was performed using an OracleBio proprietary program to calculate readouts for mean nearest neighbor distances between cell populations, as well as neighborhood analysis for selected phenotypes (Figure 3).

Results

Immune cell counts, phenotypes and spatial interactions were identified within the tumor and stroma ROI *per* core. Data included total and negative cell phenotype counts, cell density in tumor and stroma, as well as average cell distances between specified phenotypes and neighboring spatial interactions in each of the 36 cores in the TMA set.

Immune cell subsets quantified included FoxP3$^+$, CD8$^+$/PD-1$^+$, CD8$^+$/FoxP3$^+$/PD-1$^+$ and CD68$^+$/PD-L1$^+$. Tumor cells of interest included PanCK$^+$ and PanCK$^+$/PD-L1$^+$ (Figure 4). Results indicated single FoxP3 *per* mm^2 was significantly lower in the tumor ROI of the R group vs. the NR group (P≤0.05). A trend was observed in the ratio between CD8 (single and PD-1 dual combined populations) and FoxP3 (single population), where there was a higher proportion of CD8 phenotypes in both tumor ROI and stroma ROI of the R group vs. the NR group. Spatial interactions between phenotypes varied across individual cores and, although trends were observed, no significant differences were found between the R group and the NR group (Figure 3).

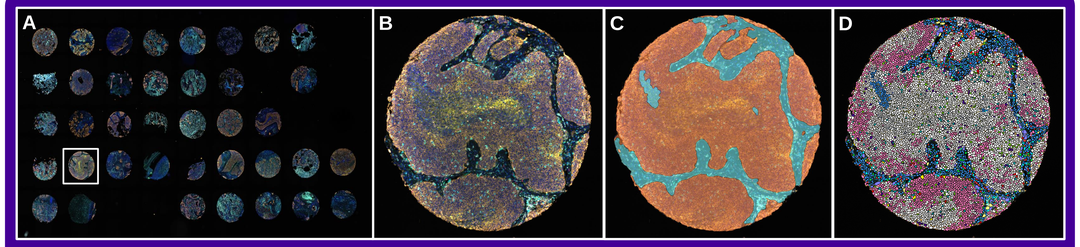

Figure 1: A. NSCLC TMA overview (n=38 cores). B. 6-plex multiplex marker staining of a whole core. C. Tumor (Orange) and Stroma (Cyan) classifier segmentation. D. Whole core cell analysis overlay.

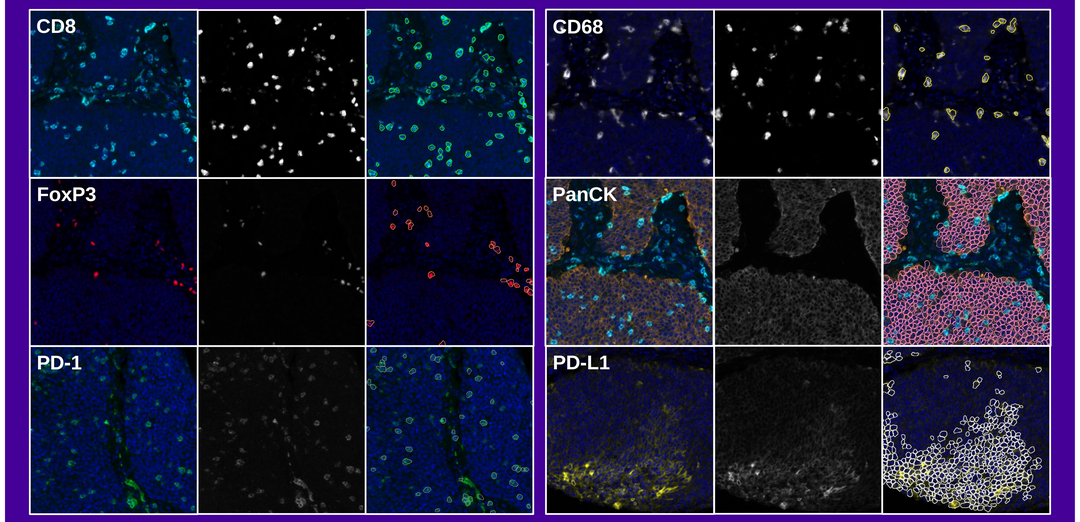

Figure 2: Exemplar staining from a 6-plex multiplex panel with corresponding analysis features and cell detection overlays. CD8 and CD68 positive cells were detected using features derived from deep learning training. FoxP3, PanCK, PD-1, and PD-L1 positive cells were detected from the raw intensity feature.

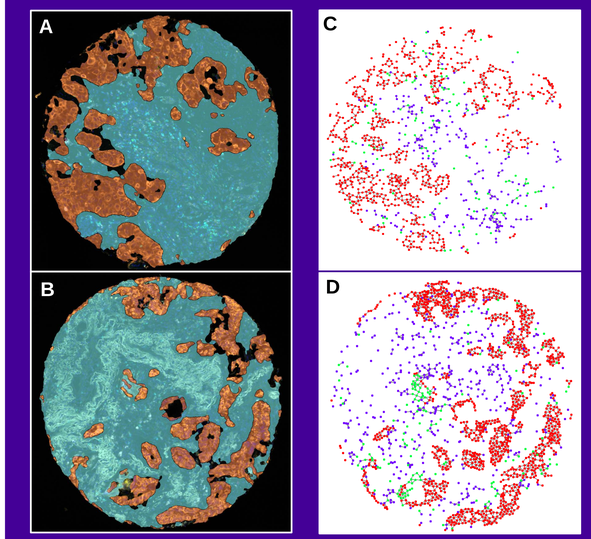

E

Spatial Interaction	Average Mean Nearest Neighbor Distance (µm)	
	Responders	Non-Responders
CD8+PD-1+/- (Stroma) to FoxP3+ (Stroma)	101	53
CD8+PD-1+/- (Stroma) to CK+PD-L1+/-(Tumor)	55	71

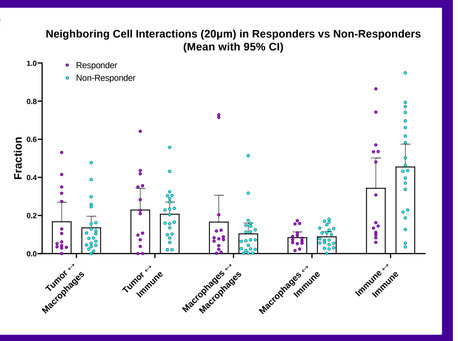

Legend: Tumor ROI Stroma ROI Phenotypes: Immune Tumor Macrophage

Figure 3: Neighborhood analysis performed across TMA cores (examples shown include top row: core from Responder Group, bottom row: core from Non-Responder Group). A-B: Tumor/stroma segmentation. C-D: Connectivity graph for neighboring cells within a 20 µm radius. E: Example phenotype - phenotype average distance within ROI F: Immune, tumor cell and macrophage phenotype interactions (within a 20µm radius).

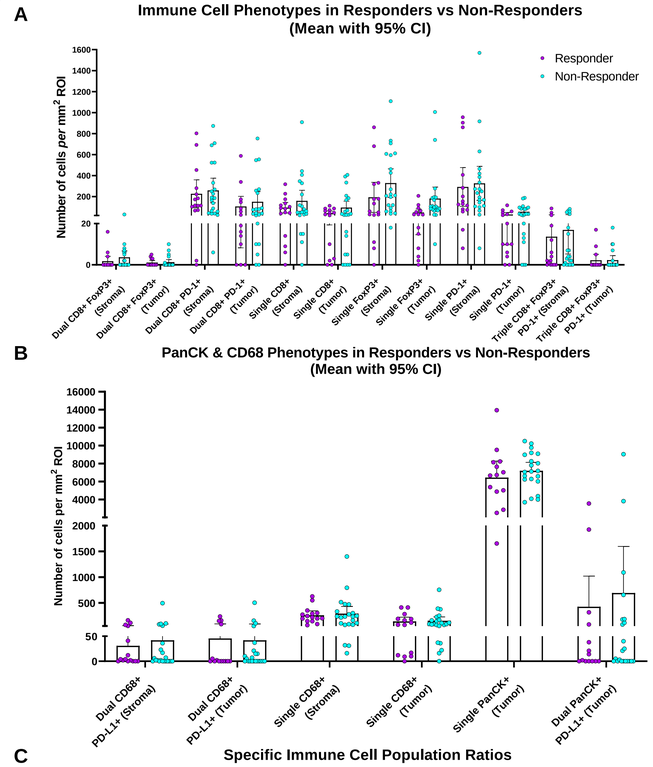

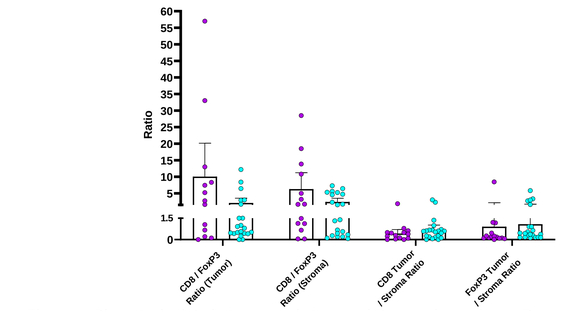

Figure 4: Phenotypic data in tumor and stroma of Responder and Non-Responder cores including (a) immune cell phenotypes, (b) PanCK and Macrophage phenotypes and (c) specific immune cell populations.

Conclusions

The combination of high quality, spatial phenotyping data provided by the PhenoCode Signature Panel, coupled with Deep Learning quantitative image analysis techniques, enables detailed characterization of the complex cellular interactions, at both the functional and spatial level, within the TME of IO-treated NSCLC tissue. This study further highlights the importance of a robust technical workflow to deliver optimal staining, imaging, cell detection and phenotyping paving the way to develop spatial signatures for responders vs non-responders in the future.

OracleBio AKOYA BIOSCIENCES®